PHYSICAL REVIEW B VOLUME 11, NUMBER 4 15 FEBRUARY 1975

Electronic structure and optical properties of 3*C*-SiC[†]

A. R. Lubinsky and D. E. Ellis
Department of Physics, Northwestern University, Evanston, Illinois 60201

G. S. Painter
Metals and Ceramics Division, Oak Ridge National Laboratory, Oak Ridge, Tennessee 37830

(Received 8 April 1974)

The electronic energy bands and wave functions of cubic 3*C*-SiC have been calculated in the first-principles Hartree-Fock-Slater model, making use of the discrete variational method. A comparison is made between experimental optical data, calculated indirect transitions, and theoretical results for $\epsilon_2(E)$ and reflectivity. The valence-band density of states is found to be in reasonably good agreement with x-ray emission spectra.

I. INTRODUCTION

The physics of silicon carbide and the possibilities of its use in device design have been subjects of considerable interest for the past decade.[1] This material is characterized by a combination of electrical, thermal, and chemical properties that make it very attractive for use in device applications for reactor and semiconductor technology. Although crystal-growth problems have limited the development of SiC as a useful technological material, its relevant electrical characteristics appear to qualify it as a more promising material for electronic device applications than Si and Ge.[2] In addition, its strong chemical bonding and physical stability are favorable for the development of devices which must withstand radiation and other severe environments. In view of the wide range of interesting properties of SiC and the importance of a comprehensive understanding of the electronic structure for possible advances in device development, we were motivated to study the electronic structure of cubic SiC within a Bloch linear-combination-of-atomic-orbitals (LCAO) band formulation.[3]

Previous first-principles treatments within this scheme for other group-IV crystals, viz, graphite and diamond, have yielded good agreement with experiment and lead us to expect that SiC can also be adequately described. In addition to the usual energy dispersion relations that characterize the overall electrical and optical behavior of the crystal, a well-converged LCAO calculation provides solutions which are convenient for further investigations, e.g., related to the bonding properties of the solid. The calculation reported here is part of a continuing study within this framework of the electronic structure of the carbides.

II. METHOD

To carry out this calculation, we used the discrete variational method[3] (DVM), a technique which has been successfully applied in first-principles LCAO band-structure treatments for several covalent and ionic crystals.[4,5] Silicon carbide is a covalently bonded crystal, and here we expand solutions as linear combinations of Bloch functions, in the manner of the LCAO method. In this calculation a basis set of 27 trial functions was constructed from atomic Slater-type orbitals corresponding to 9 carbon *s* and *p* functions and 17 silicon *s*, *p*, and *d* states. The Hamiltonian used is within the Hartree-Fock-Slater one-electron effective exchange scheme assuming crystal periodicity. The crystal potential was formed by the superposition, for each numerical integration point within the unit cell, of neighboring atomic Coulomb and charge-density contributions. No further approximations were imposed on the symmetry and spatial dependence of the potential and charge density. The statistical $\rho^{1/3}$ exchange term[6] was generated directly from the local charge density at each integration point.

Our previous investigations of the effects of linear exchange scaling through a parameter "α" have indicated a relative insensitivity of the band gaps in covalent crystals. Here, however, we find the indirect absorption edge to be appreciably affected (see Fig. 1) since the valence and conduction bands shift nonuniformly. In this treatment we use the Kohn-Sham[7] exchange parameter of $\alpha = 2/3$ since this gives an indirect transition threshold near the observed value. Other choices for α (e.g., the X_α values[8] are close to 2/3) could have been used with much the same results; however, an "optimum" α value should probably be determined in a self-consistent-field model of the crystal.

III. RESULTS

A. Band structure

The energy bands for cubic SiC calculated with this full crystal potential appear in Fig. 1. There is an interesting similarity between the results shown here and our previously published energy

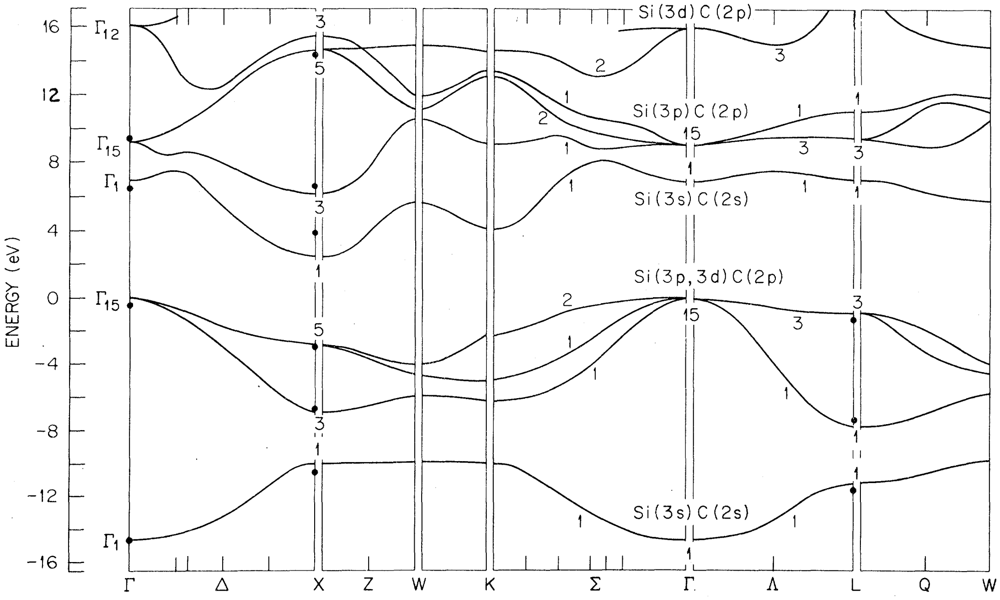

FIG. 1. Band structure of 3*C*-SiC, calculated with Kohn-Sham exchange. Dots at Γ, *X*, and *L* indicate shift of levels with full Slater exchange. The dominant atomic orbital character is indicated at Γ.

bands of diamond.[5] Certain corresponding states bear different symmetry labels and the quantitative features are not the same, but comparison of the band structures clearly shows the splittings of levels that arise from the loss of the symmetry operation of inversion through the bond center between two atoms in a cell in going from two carbons per unit cell to a carbon and a silicon. As a consequence, the valence band of SiC is separated into two parts by the lifting of degeneracy, e.g., at the *X* and *W* points.

The calculated valence bands of SiC are roughly 30% narrower (~6.5 eV) than those obtained for diamond,[5] yet wider than those presented for silicon by Chaney *et al.*[9] by about 3.5 eV. This trend follows that expected from considerations of the free-atom orbital character of the pertinent wave functions, and in Fig. 1 we denote the atomic orbital parentage at the zone center levels. In order of increasing energy with valence signified by v and conduction by c, the major components for each level are Γ_{1v}–C(2s), Γ_{15v}–C(2p), Γ_{1c}–Si(3s), Γ_{15c}–Si $\times$(3p), and Γ_{12c}–Si(3d).

Diamond is characterized by an (calculated) indirect transition threshold of about 5.4 eV involving the zone-center valence-band edge and a point about 0.7 along Δ from Γ to *X*. In SiC this conduction-band minimum has moved to the point *X* and lies only 2.4 eV above the valence-band edge,[10,11] thus typifying the material as a large-gap semiconductor. The conduction minimum at *X* also supports an indirect transition from the L_{3v} valence-band state, and a local conduction minimum at *K* indicates the possibility of a 4.2 eV indirect transition from the zone center.[11] The calculated threshold for direct transitions is about 5.3 eV and occurs at the point *X* in the Brillouin zone.

It is also interesting to compare the band structures of 3*C*-SiC and diamond with regard to direct transitions at various points in the Brillouin zone which may contribute to structure in the optical absorption. The optical absorption in diamond is dominated by a single large peak at 12.2 eV. Such a large peak in ϵ_2 cannot be ascribed to a single critical-point transition, but must arise from transitions in a similarly large fraction of the reduced zone. In diamond we find that the transitions X_4-X_1, $\Sigma_2-\Sigma_3$, $L_{3'}-L_3$, and $L_{3'}-L_1$ are all among those contributing to the main peak. The contribution from transitions near the point *L* will be especially important in this case because we find the three lowest conduction bands are all very close, being split less than 0.5 eV along the symmetry line ΓΛ*L* in diamond.

In SiC we find two main peaks in ϵ_2, and once again transitions near the *L* point are important. Examination of the band structure of SiC shows that the highest valence and lowest two conduction bands are quite flat along ΓΛ*L*, each varying by less than 1.0 eV. In addition, in contrast to the case of diamond, the two lowest conduction bands are not contiguous along this symmetry line but are split by about 2 eV. In SiC we find that the transition $L_{3v}-L_{1c}$ as well as transitions at points along Λ, Σ, and Δ contribute to the first peak in ϵ_2, at 8.2 eV. The transition $L_{3v}-L_{3c}$ is now associated with a second peak in ϵ_2, about 2 eV higher. Transitions at the X point are responsible for the direct threshold in SiC. Additional structure in ϵ_2 above the direct threshold arises from transitions about the Γ and K points. Our subsequent presentation of the calculated optical properties of 3C-SiC in Sec. III C verifies these qualitative observations.

B. Density of states

The density of states of 3C-SiC was calculated by direct fitting and numerical integration procedures described in detail in a previous article.[5] Fourier-series representations of each of the four highest valence bands (labeled bands 1–4 here) and the four lowest conduction bands (bands 5–8) were obtained by least-square fitting the energy-band data at 45 wave vectors distributed uniformly throughout the irreducible wedge of the Brillouin zone, using symmetrized sums of plane waves[12] as the fitting functions. With 20 fitting functions per band, rms errors of approximately 0.05 eV in the valence bands and 0.12 eV in the conduction bands were obtained, while undesirable oscillatory behavior in the fits was kept to an acceptably minimal level. We obtained the density of states in each band

$$d_j(E) = \frac{2}{(2\pi)^3} \int d\vec{k}\, \delta(E_j(\vec{k}) - E) \qquad (1)$$

in a histogram representation by irrational vector sampling[13] using 25000 sampling points in the Brillouin zone and a histogram width of 0.02 a.u. (~0.55 eV).

The results for the total density of states $D(E) = \sum_j d_j(E)$ are presented in Fig. 2. The valence-band density of states is separated into two parts by a 1.6-eV gap. The higher peak, due to bands 2–4, is 8.2 eV wide, and the lower peak, due to band 1, is about 5.5 eV wide. The width of the higher structure compares well with the first-principles OPW result (7.8 eV) of Herman, Van Dyke, and Kortum.[14] In contrast, the pseudopotential calculation of Hemstreet and Fong[15] yields a considerably larger width (11.6 eV) for this part of the valence bands.

Structure in the valence-band density of states may be compared with soft-x-ray emission data. Although complete interpretation of experimental intensity spectra would involve consideration of k-dependent transition probabilities as well as relaxation effects, the energy location of experimental structure can be related to the location of corresponding structure in the theoretical density of states. A superposition of the K and $L_{2,3}$ emission intensity spectra of Wiech[16] appears as the smooth curve in Fig. 2. Four pieces of structure are noted: a large peak, an edge, a narrow peak, and another smaller peak, in order of decreasing energy. The latter three are spaced 2.3, 4.6, and 9.2 eV below the center of the first large peak. The calculated valence-band density of states has a large peak due to bands 3 and 4, and edge approximately 2.2 eV below the center of this peak, a narrow peak 4.6 eV lower due to band 2, and a peak due to band 1, 8.4 eV below the first peak. The calculated density of states for the occupied bands is in qualitative agreement with the general shape of the experimental soft-x-ray emission spectra, and in reasonable quantitative agreement with the spacing in energy of the important experimental structure.

The ratios of the peak heights C_2, A, and B (Fig. 2) best match the experimental data based on K-to-L intensity ratios of 2 : 1 or 3 : 1 rather than 1 : 1. This is as one would qualitatively expect for the tetrahedral bonding in the solid which favors an sp^3 over an s^2p^2 atomic configuration, since K and L emission sample p and s character of the bands, respectively. The I_K/I_L intensity ratio essentially measures the ratio of Si-p to s character (averaged over $\vec{k}$ at a given energy) in the valence bands; by examining our calculated eigenfunctions, we find this to be an increasing function of the energy. If we average over the entire valence bandwidth, the I_K/I_L ratio should approach 3.

In Table I we compare the valence bandwidths and the energy gap between the valence bands with the x-ray emission results of Wiech.[16] Although the experimental bandwiths are somewhat sensitive to the details of extrapolation techniques and there are slightly differing results in the literature,[17–19] the theoretical density of states alone yields a total bandwidth (15.2 eV) which is 1.0–2.0 eV too narrow. Considering similar studies that have been made for diamond[5] and graphite,[20] this appears to

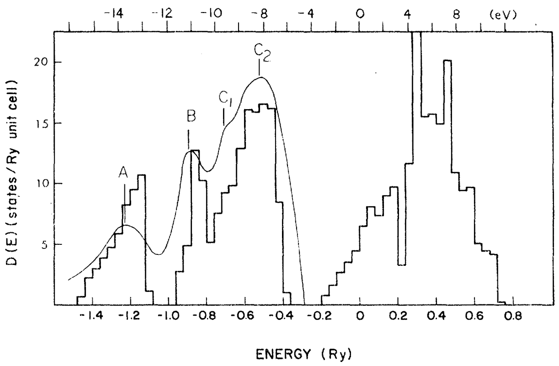

FIG. 2. Density of states in valence and lowest conduction bands of SiC, calculated from the DVM band structure. The smooth curve is the experimental superimposed K and $L_{2,3}$ emission bands for an intensity ratio of 2 : 1 as reported by Wiech (Ref. 16).

TABLE I. Valence bandwidths and gap in $3C$-SiC (eV).

Experiment[a]	Theory	Feature
9.0–9.5	8.2	C_2
4.5–6.0	5.5	A
2.0–3.0	1.6	gap

[a] Reference 16.

be a characteristic feature of first-principles density of states when compared with data from soft-x-ray emission[21] and x-ray photoemission[22,23] (XPS) band-probe experiments.

C. Wave functions and charge density

Several typical valence-band wave functions are shown in Fig. 3, plotted along the [111] bond direction. At the high-symmetry points considered (Γ, X, L) the eigenfunctions show very clearly the atomic composition and bonding character of Si and C constituents. For example, the bottom of the valence bands (Γ_1) begins as a bonding combination of Si-3*s* and C-2*s*, transforms into the Si-3*p*, C-2*s* mixture at X_1, and shows the more general hybrid Si-3*sp*, C-2*s* composition at L_1. The states Γ_{15}, X_3, and L_1 (dashed curves) were similarly selected to show the bonding character of C-2*p* combinations with Si-3*s* and Si-3*p*. Finally, we see that the X_5 state displays the rather simple combination of Si-3*p* and C-2*p* character found near the top of the valence bands.

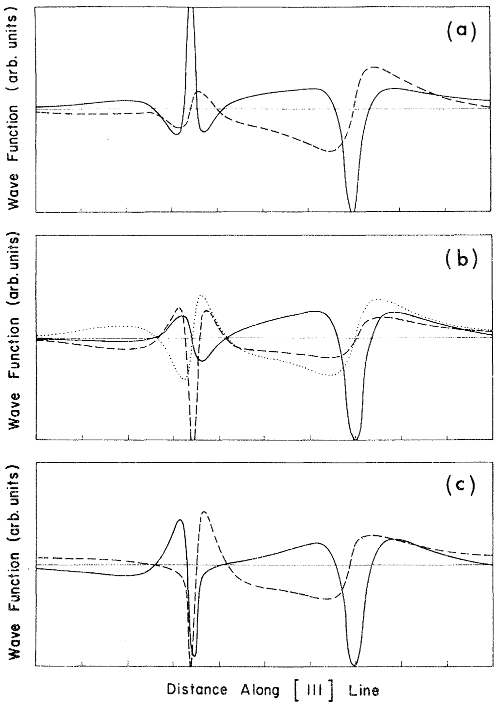

FIG. 3. SiC valence-band wave functions plotted along [111] bond direction: (a)Γ_1 (solid line), Γ_{15} (dashed); (b) X_1 (solid), X_3 (dashed), X_5 (dotted); (c) L_1 (solid), second L_1 (dashed).

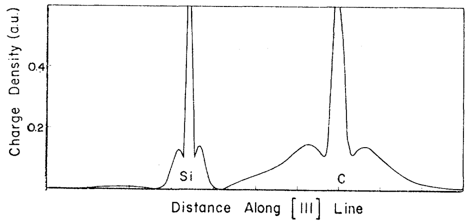

FIG. 4. SiC crystal valence charge density plotted along [111] bond direction, constructed by averaging densities calculated at symmetry points Γ, *X*, and *L*.

It is noteworthy that the outer maximum of the free-atom Si-3*s*3*p* shells lies practically in the middle of the SiC bond. A comparison of superimposed free-atom densities with the crystal valence charge density calculated from our eigenfunctions (plotted along the [111] direction in Fig. 4) shows that a relatively small amount of charge transfer has taken place. In fact, the bond formation can be rather well described by a polarization of the Si density along the bond directions and a radial expansion of the carbon valence density. This interpretation of the bonding mechanism is made clear by reference to Fig. 5; here the valence charge transfer ρ_v(crystal) − ρ_v(superimposed atoms) is given along the [111] bond direction. It is evident that no really useful definition of ionicity can be found here, since the valence densities of either species overlap and interact strongly. Since the bond formation is seen to occur mostly by internal rearrangement of the atoms, we conclude that our initial choice of potential (based on free-atom densities) is satisfactory. While fully self-consistent calculations would be interesting, we believe that the net changes in band structure and wave functions would not be large.

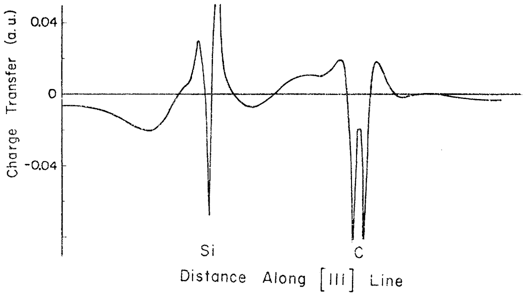

FIG. 5. SiC charge transfer plotted along [111] bond direction. The difference ρ_v (crystal) $-\rho_v$ (superimposed atoms) is shown.

The sensitivity of band energies and wave-function character to changes in basis set was also investigated, within the framework of the model potential treated here. Successively larger sets were treated, by augmenting the Slater-type orbital basis given in Table II with s-, p-, and d-type orbitals on *both* silicon and carbon sites. The valence and first four conduction bands were found to be remarkably well determined by the smaller (27-function) basis. For example, the "best" (46-function) basis, including efforts to optimize orbital-screening parameters, yielded a change of less than 0.1 eV in the direct-band gap, and similarly small changes in other features of these bands. The additional variational freedom was, however, apparent in sizable shifts of the higher conduction bands, where Si-$3d$ character becomes important.

TABLE II. STO basis functions.

Site	nl	ξ	Site	nl	ξ
Si	$1s$	13.57	C	$1s$	5.67
	$2sp$	5.00		$2sp$	2.60
	$3sp$	1.75		$2sp$	1.40
	$3spd$	1.35			

D. Optical properties

The direct-interband-transition contribution to the optical absorption, expressed as $\epsilon_2(E)$, the imaginary part of the dielectric function, can be compared with experimental reflectivity and absorption measurements and affords an important test of theoretical band-structure models in insulators and semiconductors. Hemstreet and Fong[24] have used the empirical pseudopotential method to calculate ϵ_2 and the reflectivity for $3C$-SiC. Herman, Van Dyke, and Kortum[14] earlier presented a claculation of the optical structure, but were hindered by the lack of experimental information in constructing an "empirically refined model." Structure in the optical absorption from the indirect threshold up to the direct gap in $3C$-SiC is known experimentally from the measurements of Choyke, Hamilton, and Patrick,[10,11,25] but the experimental situation in the fundamental absorption region, above the direct threshold, is less clear. The normal incidence reflection of $3C$-SiC from 3 to 13 eV has been measured by Wheeler[26] and also by Belle *et al.*[27] in the range 1–12 eV. The experimental reflectivities have not been used to derive ϵ_2 spectra. Also, the two sets of reflectivity data differ considerably in several important respects, further complicating detailed comparisons with theory and pointing out the need for more experimental work in this area.

1. Indirect absorption

The optical properties of $3C$-SiC in the energy range from 2.4 up to 6.0 eV are dominated by the effects of indirect electronic transitions. Although we do not attempt to calculate structure in the optical absorption due to phonon-assisted transitions, we can compare the sizes of the important indirect gaps found in our calculation with the experimental results, which is done in Table III. The first entry in the table is the experimentally best known detail of the optical structure, the first indirect gap. (The experimentally determined quantity is the "exciton energy gap," which is the usual gap minus the binding energy of the exciton created in the transition.) For a reduced exchange coefficient of $\frac{2}{3}$, the calculated energy gap is in very good agreement both with experiment and with previous first-principles theoretical results[14] using this exchange value. The exchange coefficient here is used as a parameter in the spirit of the empirical pseudopotential calculations, in which the size of this gap is also viewed as a feature of the band structure to be fit by adjustment of parameters. The assignment of the electronic transition responsible for the onset of indirect absorption is in agreement with earlier work, except that of Junginger and van Haeringen,[28] who studied the energy-band structure of four polytypes of SiC by the empirical pseudopotential method, and whose labelling of the conduction band states at X in $3C$-SiC differs from our own and that of other authors. Our assignment of the second edge at 3.55 eV to L_{3v}-X_{1c} transitions is also in agreement with earlier work. The first attempt to identify the edge at 4.20 eV was made in the pseudopotential calculation of Hemstreet and Fong,[15,24] where this structure was ascribed to the transition Γ_{15v}-L_{1c}. Our calculated band structure does not support this assignment; we find the state L_{1c} at a considerably higher energy with respect to the conduction-band minimum at X. We instead assign this edge to indirect transitions from the valence-band maximum at Γ to conduction-band states associated with a secondary minimum at K with an energy gap of 4.3 eV. Experimental results[29] for the $2H$-SiC polytype reveal an indirect threshold of 3.3 eV between the zone center and the conduction-band minimum at K. The K point in the reciprocal space of the $3C$-SiC lattice lies very close to the K point in the hexagonal Brillouin zone of $2H$-SiC (see the Appendix of Ref. 14); thus it is not surprising to find this local minimum in the present calculation.

2. Direct transitions and oscillator strengths

We calculate interband contributions to the imaginary part of the dielectric tunction $\epsilon_2(E)$ in the approximation[30]

TABLE III. Optical gaps in 3C-SiC (eV)

Experiment	Reference	Theory	Transition
2.39	23, 25	2.5	Γ_{15v}-X_{1c}
3.55	25	3.4	L_{3v}-X_{1c}
4.20	25	4.3	Γ_{15v}-K_c
3.05[a]	24	3.8	X_{1c}-X_{3c}

[a] Donor induced gap.

$$E\epsilon_2(E)=\frac{e^2h^2}{m}\sum_{i,j}\frac{1}{(2\pi)^3}\int d\vec{\mathrm{k}}\,f_{ij}(\vec{\mathrm{k}})\,\delta(E_{ji}(\vec{\mathrm{k}})-E)\;, \quad (2)$$

where

$$f_{ij}(\vec{\mathrm{k}})=\frac{2\,|\langle\vec{\mathrm{k}},i\,|\,\vec{\mathrm{p}}\,|\,\vec{\mathrm{k}},j\rangle|^2}{3mE_{ji}(\vec{\mathrm{k}})} \quad (3)$$

is an interband oscillator strength connecting valence band i and conduction band j at the wave vector $\vec{\mathrm{k}}$, and $E_{ji}(\vec{\mathrm{k}})$ is the energy difference at $\vec{\mathrm{k}}$. The wave functions were obtained from the DVM procedure as a linear combination of Bloch functions, which were, in turn, constructed from Slater-type orbitals (STO's) centered at atomic sites. A total of 27 STO's were used, as shown in Table II. We found that valence and first conduction bands (bands 1–8) were not changed significantly when the basis was augmented; however, a more extended basis would be desirable to allow description of features of the higher conduction bands. The momentum matrix elements were calculated using $\vec{\mathrm{k}}$ interpolation and integration methods described previously.[5] We obtain the contributions to $\epsilon_2(E)$ from each of 16 band pairs in a histogram representation. The histogram width chosen for the final calculation was 0.015 a.u. (~0.4 eV), and $N=25\,000$ sampling points were used. In addition, computational accuracy of structure in the interband densities of states was tested in higher resolution calculations with N up to 50 000 points.

To investigate the effects of the k-dependent oscillator strengths, we also calculated $\epsilon_2(E)$ in a constant-oscillator-strength approximation:

$$E\,\epsilon_2(E)=\frac{e^2h^2}{m}\sum_{i,j}\langle f_{ij}\rangle\, d_{ij}(E)\;, \quad (4)$$

where $\langle f_{ij}\rangle$ is a k-averaged oscillator strength connecting bands i and j, and $d_{ij}(E)$ is the corresponding interband density of states. This compares with the expression (2), which we write in the form

$$E\,\epsilon_2(E)=\frac{e^2h^2}{m}\sum_{i,j}f_{ij}(E)\,d_{ij}(E)\;, \quad (5)$$

with

$$f_{ij}(E)=\frac{\int d\vec{\mathrm{k}}\,f_{ij}(\vec{\mathrm{k}})\,\delta(E_{ji}(\vec{\mathrm{k}})-E)}{\int d\vec{\mathrm{k}}\,\delta(E_{ji}(\vec{\mathrm{k}})-E)}\;, \quad (6)$$

in order to make explicit the effects of the oscillator strengths on the energy dependence of ϵ_2.

The real part of the dielectric function, given by

$$\epsilon_1(E)=1+\frac{2}{\pi}\,\frac{e^2h^2}{m}\sum_{i,j}\frac{1}{(2\pi)^3}\,\mathcal{P}\int\frac{d\vec{\mathrm{k}}\,f_{ij}(\vec{\mathrm{k}})}{E_{ji}^2(\vec{\mathrm{k}})-E^2}\;, \quad (7)$$

is related to the imaginary part by Kramers-Kronig transformation. Rather than calculating ϵ_1 directly, we obtain it from ϵ_2 using the integral transform. To carry out this procedure, $\epsilon_2(E)$ must be known for all energies; for this purpose we use a high-energy extrapolation of the form

$$\epsilon_2=\beta E/[E^2+(h/\tau)^2]^2\;.$$

This form has been used by Ehrenreich and Phillip[31] for empirical fitting purposes in semiconductors in the energy region where most of the interband oscillator strength has been exhausted. Here τ represents in an average way lifetime broadening effects, and we choose β for continuity with the calculated $\epsilon_2(E)$ at that energy at which transitions to states higher in energy than those we have explicitly considered begin.

Once ϵ_1 and ϵ_2 are known, other optical constants may be obtained, and here we use Fresnel's relation

$$R=\frac{1+(\epsilon_1^2+\epsilon_2^2)^{1/2}-[2\epsilon_1+2(\epsilon_1^2+\epsilon_2^2)^{1/2}]^{1/2}}{1+(\epsilon_1^2+\epsilon_2^2)^{1/2}+[2\epsilon_1+2(\epsilon_1^2+\epsilon_2^2)^{1/2}]^{1/2}} \quad (8)$$

to calculate the reflectivity as a function of energy in order to make a direct comparison with the experimental data.

The energy-dependent oscillator strengths connecting the three most important band pairs contributing to ϵ_2 are shown in Fig. 6, along with the k-averaged values. These functions, when multiplied by the corresponding interband densities of states according to Eq. (5), give the contributions to ϵ_2 from each band pair, which are shown in Fig. 7. It is seen that the oscillator strength for transitions between bands 4 and 5 decreases steadily with energy, crossing its average value near 8 eV, close to the energy of the first peak in ϵ_2 for 3C-SiC. Inclusion of these oscillator strengths will then increase the calculated ϵ_2 on the low-energy side of the first ϵ_2 peak, decrease it at higher energies, and shift the peak location slightly to lower energy. The 3-5 oscillator strengths exhibit somewhat more structure, decreasing at low energies, but then increasing again near 8 eV before falling below the average value at higher energies. Their inclusion will increase ϵ_2 at low energies, increase and sharpen the 3-5 contribution to the peak near 8 eV, and decrease ϵ_2 at higher energies. It is seen that the 4-6 oscillator strengths exceed their k-averaged values only in the neighborhood of 10 eV, near the second peak in ϵ_2, falling off at higher energies. Their inclusion will increase the 4-6 contribution to the second peak and will diminish the relative strength of structure due to this band pair at higher energies.

3. *Imaginary part of the dielectric function*

From Fig. 7 it is seen that, although 4-5 transitions contribute most strongly to ϵ_2 in 3*C*-SiC, 3-5 and 4-6 transitions are also important. In particular, 4-6 transitions are largely responsible for the second ϵ_2 peak, and 3-5 transitions also contribute noticeable structure. This is in contrast to the situation in diamond,[5] where the optical spectrum, particularly near the main peak, is dominated by the effects of 4-5' transitions. This rearrangement of oscillator strength in passing from the strongly covalent crystal to the somewhat more ionic case of 3*C*-SiC is in general agreement with theoretical expectations.[32] It is found that the first ϵ_2 peak is due to 4-5 and 3-5 transitions, roughly in the proportion 70% and 30%. Several interband pairs contribute to the second peak, the most important being 4-6 (60%), 3-6 (20%), and 3-5 (10%) transitions. In Fig. 8, the theoretical ϵ_2 calculated from all 16 pairs of bands is shown, along with ϵ_2 in the constant-oscillator-strength approximation, to demonstrate the effects of inclusion of the *k*-dependent matrix elements. The overall magnitude of these effects is noticeable, but considerably less pronounced than for diamond.

Although the position of peaks in ϵ_2 and the reflectivity are not strictly comparable, we have summarized important features in the calculated $\epsilon_2(E)$ and experimental reflectivity data in Table

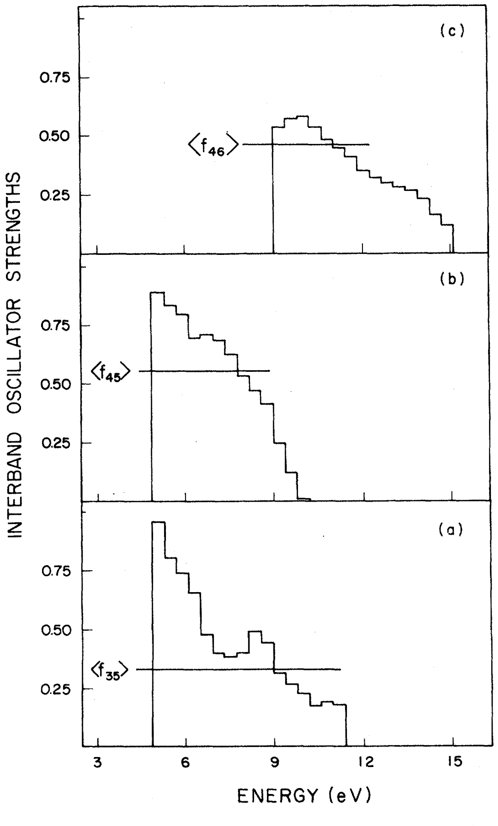

FIG. 6. Important interband oscillator strengths, given as a function of transition energy: (a) $f_{35}(E)$, (b) $f_{45}(E)$, (c) $f_{46}(E)$. Horizontal lines indicate $\vec{k}$-averaged values $\langle f_{ij}\rangle$.

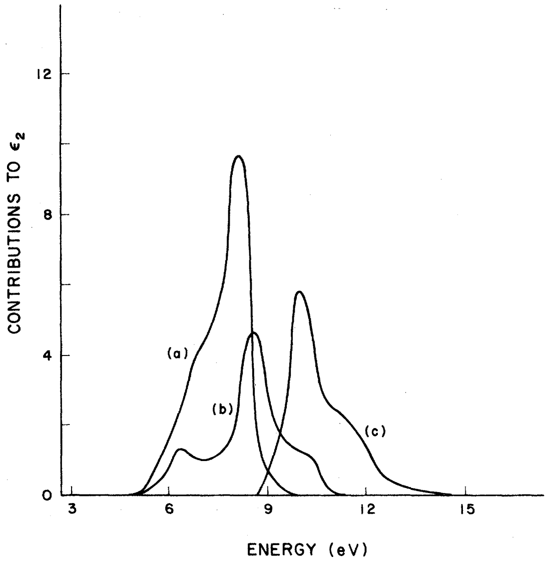

FIG. 7. Individual valence → conduction-band pair contributions to $\epsilon_2(E)$: (a) $4\rightarrow5$, (b) $3\rightarrow5$, (c) $4\rightarrow6$.

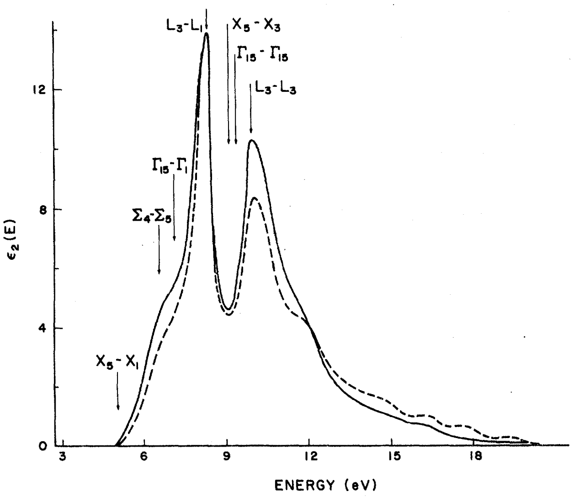

FIG. 8. Imaginary part of the dielectric function, $\epsilon_2(E)$, including transitions from valence bands (1, 2, 3, 4) to conduction bands (5, 6, 7, 8). Dashed line is $\vec{k}$-averaged oscillator strength approximation; solid line is the result with $\vec{k}$ dependence of f_{ij} included. Positions of transitions at several symmetry points in the Brillouin zone are indicated.

TABLE IV. Comparison of structure in ϵ_2 with experimental reflectivity data of Wheeler (Ref. 26) (energy in eV).

Experiment	Theory	Feature
6.0	6.7	Leading shoulder
7.8	8.2	Main peak
9.0	9.1	Minimum
9.7	9.9	Broad peak
none	11.2	Weak shoulder

IV. The resolution of our calculation introduces an uncertainty of 0.2 eV or less in the quoted location in energy of any structure in ϵ_2. In Fig. 8, structure in the theoretical ϵ_2 (including matrix elements) is observed at 5.3, 6.6., 8.2, 9.1, 9.9, and 11.2 eV. The energies of several important transitions at symmetry points in k-space are noted on the figure. We find that the direct threshold arises from X_{5v}-X_{1c} transitions at 5.3 eV with large oscillator strengths. The calculated ϵ_2 rises rapidly with energy up to 6.4 eV, where 4-5 transitions along Σ and near the point K contribute strongly. A shoulder is observed at 6.7 eV which is due to a sharp edge in the 3-5 interband contribution to ϵ_2. This edge is due to transitions near the point X, combined with a sharp decrease in oscillator strengths for these transitions near 6.5 eV. The absorption rises again as zone-center Γ_{15v}-Γ_{1c} transitions contribute, reaching a peak at 8.2 eV. Although L_{3v}-L_{1c} transitions at 8.1 eV contribute strongly to this peak, and inspection of 4-5 energy contour plots reveals an M_1 critical point on Δ near ($-$0.3, 0, 0) $(2\pi/a)$ at 8.1 eV and an additional M_2 critical point on Σ near (0.36, 0.36, 0) $(2\pi/a)$ at 8.4 eV, we emphasize that states in a large volume of the Brillouin zone are participating in transitions at these energies and are jointly responsible for the size of the first peak in ϵ_2. There is a sharp edge in the 4-5 interband density of states at 8.6 eV, and the calculated ϵ_2 falls off rapidly on the high-energy side of the first peak, reaching a minimum at 9.1 eV. The absorption begins to rise again with the onset of 4-6 transitions, beginning with the X_{5v}-X_{3c} and Γ_{15v}-X_{15c} transitions, and it reaches a peak at 9.9 eV. In addition to the critical transition L_{3v}-L_{3c} at 9.9 eV, 4-6 and 3-6 transitions in a large volume of the Brillouin zone, particularly in regions around the L point and along the lines Σ and Δ, contribute to this peak. Regarding the doublet structure near 10 eV observed in previous calculations[14,24] and in the experimental data of Belle *et al.*,[27] we do find an additional peak in the 3-5 interband density of states at 10.5 eV. The 3-5 oscillator strengths are very small at these energies, however, and this structure would appear only very weakly if at all in a higher-resolution ϵ_2 calculation. The calculated ϵ_2 falls off quickly at higher energies, with a weak change in slope around 11.2 eV which is due to 4-7 transitions.

4. *Reflectivity*

In general, structure in ϵ_2 is not directly reproduced in the reflectivity; the process of deriving one from the other introduces changes in line shape as well as shifts in the location of structure. Peaks in ϵ_2 may be shifted by several tenths of an eV to higher energy in $R(E)$, for example. Also, even though indirect transitions are not expected to introduce singular structure into the reflectivity,[33] their neglect in the theoretical ϵ_2 will hinder direct comparison of the derived $R(E)$ with experiment at low energies.

In Fig. 9 are shown the theoretical reflectivity $R(E)$ (curve c) derived from the calculated ϵ_2 along with the experimental data of Wheeler (curve a) and Belle *et al.* (curve b). Structure in the experimental data of Wheeler is observed at 4.6, 6.0, 7.1, 7.75, 8.3, and 9.7 eV. The structure at 4.6 eV is not reproduced in other measurements,[11,27] nor do we find any evidence for it in our calculation. The important features of the experimental data are the main peaks near 7.8 and 9.7 eV and the structure near 6.0 eV, which has been associated with the onset of direct transitions. The theoretical R is observed to rise smoothly up to about 6.3 eV, where a shoulder is found. Another change in slope occurs at 7.1 eV, and R rises to a peak at 8.3 eV, corresponding to the first large ϵ_2 peak. There is a large dip at 9.1 eV, and R rises again to about 10.7 eV, where a shoulder

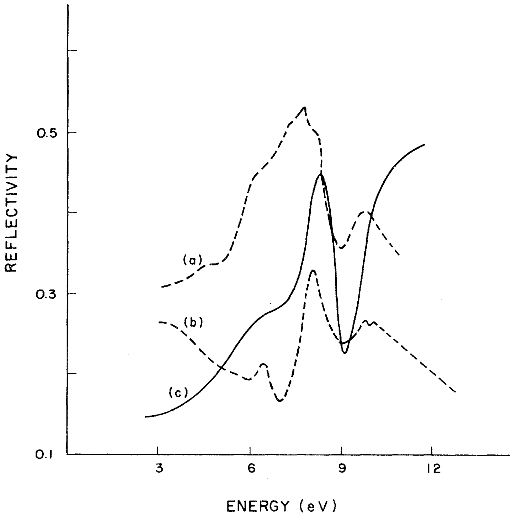

FIG. 9. Comparison of experimental reflectivity by (a) Wheeler (Ref. 26), and (b) Belle *et al.* (Ref. 27) with the calculated value (c).

is found, corresponding to the second peak in ϵ_2. Although more definitive data would be helpful for comparison, there is some disagreement between the shape of the calculated $R(E)$ and experiment, particularly at higher energies. The shoulder, main peak, and minimum are in reasonable agreement with the positions of the experimental structure; however, instead of a second peak, as found experimentally, we obtain only a shoulder (followed by yet another rise before decreasing at higher energy). This behavior persists regardless of the details of the ϵ_2 extrapolation that is used and appears to originate from the rapid decrease with energy in the calculated ϵ_2 above 10.0 eV, on the high-energy side of the second major peak.

The lack of closer agreement between the calculated reflectivity and the measured curves is somewhat surprising in view of our experience in the qualitatively similar case of diamond. Although exchange scaling and self-consistency effects are probably more important in the present case, we have seen that a self-consistent charge rearrangement would not be expected to alter the calculated results substantially. However, the calculated structure in $R(E)$ does appear to occur at energies 0.5–1.0 eV too high compared to experiment. This disagreement worsens as one goes to higher energies.

The present ϵ_2 calculation, while in qualitative agreement in shape with the results of Herman *et al.*,[14] is in some disagreement with the empirical pseudopotential results of Hemstreet and Fong,[24] who obtain very good agreement with the reflectivity data of Wheeler.[26] While recognizing that agreement in a particular calculated property with experimental data does not uniquely define a "correct" band structure, it does appear that further refinements will be helpful in bringing the present model into closer agreement with experiment.

Finally, the ambiguity in the experimental situation above the direct threshold has been mentioned. Refinements of the present optical data in this region will be helpful in making further progress toward understanding the electronic structure of SiC.

IV. DISCUSSION

The major features of the electronic band structure of 3C-SiC, as elucidated by soft-x-ray emission, optical reflectivity, and absorption studies, have been described reasonably well in this first-principles LCAO calculation. Structure in the valence-band density of states compares well with the results of Wiech; however, the calculated bandwidth appears to be too narrow by ~2 eV. The calculated ϵ_2 is structurally similar to that previously presented for diamond, with the main differences being the existence of a double peak in SiC. This similarity follows from the resemblance of many features of the band structures of these two materials. The good agreement with experiment obtained for diamond thus leads us to expect that the theoretical ϵ_2 for SiC is reasonably accurate; however, the lack of experimental data at present prevents further assessment of this part of the calculation. Although fair general agreement exists between the location of important structure in the calculated optical constants and experiment (Table III), the location of calculated structure in the reflectivity does appear to be several tenths of an eV too high. Detailed comparison of the shape of the calculated $R(E)$ with experiment is less than satisfactory. At low energies, indirect transitions, neglected in the present calculation, will have an important effect on the experimental line shapes. At energies above the main peak in ϵ_2, disagreement is also found; the calculated $R(E)$ is systematically too large compared to experiment. It is suggested that further experiments in the energy range 4–12 eV would be helpful in resolving differences between reported data and the present calculations.

[†] Research supported by the Advanced Research Projects Agency through the Northwestern University Materials Research Center, by the Air Force Office of Scientific Research, Grant No. 71-2012, and by the U.S. Atomic Energy Commission under contract with the Union Carbide Corp.

[1] A recent survey of research on silicon carbide appears in Mater. Res. Bull. 4, S1-372 (1969).

[2] R. W. Keyes, Comments Solid State Phys. 4, 12 (1971).

[3] D. E. Ellis and G. S. Painter, Phys. Rev. B 2, 2887 (1970).

[4] G. S. Painter and D. E. Ellis, Phys. Rev. B 1, 4747 (1970); G. S. Painter, Int. J. Quantum Chem. 5, 501 (1971); P. F. Walch and D. E. Ellis, Phys. Rev. B 8, 5920 (1973).

[5] G. S. Painter, D. E. Ellis, and A. R. Lubinsky, Phys. Rev. B 4, 3610 (1970); A. R. Lubinsky, D. E. Ellis, and G. S. Painter, Phys. Rev. B 6, 3950 (1972).

[6] J. C. Slater, Phys. Rev. 81, 385 (1951).

[7] W. Kohn and L. J. Sham, Phys. Rev. 140, A1133 (1965).

[8] K. H. Schwarz, Phys. Rev. B 5, 2466 (1972).

[9] R. C. Chaney, C. C. Lin, and E. E. Lafon, Phys. Rev. B 2, 459 (1970).

[10] W. J. Choyke, D. R. Hamilton, and Lyle Patrick, Phys. Rev. 133, A1163 (1964).

[11] W. J. Choyke and Lyle Patrick, Phys. Rev. 187, 1041 (1969).

[12] J. B. Ketterson, F. M. Mueller, and L. R. Windmiller, Phys. Rev. 186, 656 (1969).

[13] D. E. Ellis, Int. J. Quantum Chem. 2, 35 (1968).

[14] F. Herman, J. P. Van Dyke, and R. L. Kortum, Mater. Res. Bull. 4, S167 (1969).

[15] L. A. Hemstreet, Jr. and C. Y. Fong, Solid State Commun. 9, 643 (1971).

[16] G. Wiech, in *Soft X-ray Band Spectra*, edited by D. J. Fabian (Academic, New York, 1968).

[17] B. Kern, Z. Phys. 159, 178 (1960).

[18] I. I. Zhukova, V. A. Fomichev, A. S. Vinogradov, and T. M. Zimkina, Fiz. Tverd. Tela 10, 1383 (1968) [Sov. Phys.-Solid State 10, 1097 (1968)].

[19] V. V. Nemoshkalenko and V. G. Aleskin, Fiz. Tverd. Tela 12, 59 (1970) [Sov. Phys.-Solid State 12, 46 (1970)].

[20] R. A. Willis, B. Fitton, and G. S. Painter, Phys. Rev. B (to be published).

[21] M. Umeno and G. Wiech, Phys. Status Solidi 59, 145 (1973).

[22] R. G. Cavell, S. P. Kowalczyk, L. Ley, R. A. Pollak, B. Mills, D. A. Shirley, and W. Perry, Phys. Rev. B 7, 5313 (1973).

[23] F. R. McFeely, S. P. Kowalczyk, L. Ley, R. G. Cavell, R. A. Pollak, and D. A. Shirley, Phys. Rev. B (to be published); we thank Dr. Kowalczyk for a preprint of this work.

[24] L. A. Hemstreet, Jr. and C. Y. Fong, Phys. Rev. B 6, 1464 (1972).

[25] Lyle Patrick and W. J. Choyke, Phys. Rev. 186, 775 (1969).

[26] B. E. Wheeler, Solid State Commun. 4, 173 (1966).

[27] M. L. Belle, N. K. Prokof'eva, and M. B. Reifman, Fiz. Tekh. Poluprovodn. 1, 383 (1967) [Sov. Phys.-Semicond. 1, 315 (1967)].

[28] H.-G. Junginger and W. van Haeringen, Phys. Status Solidi 37, 709 (1970).

[29] L. Patrick, D. R. Hamilton, and W. J. Choyke, Phys. Rev. 143, 526 (1966).

[30] H. Ehrenreich and M. H. Cohen, Phys. Rev. 115, 786 (1959).

[31] H. Ehrenreich and H. R. Phillip, in *Report of the International Conference on the Physics of Semiconductors, Exeter*, 1962, edited by A. C. Stickland (Institute of Physics and the Physical Society, London, 1962).

[32] J. C. Phillips, in *Solid State Physics*, edited by F. Seitz and D. Turnbull (Academic, New York, 1966), Vol. 18.

[33] F. Stern, in Ref. 32, Vol. 15.